MOLECULAR AND CELLULAR BIOLOGY, June 1993, p. 3370–3383
0270-7306/93/063370-14$02.00/0

Vol. 13, No. 6

Mouse Heat Shock Transcription Factors 1 and 2 Prefer a Trimeric Binding Site but Interact Differently with the HSP70 Heat Shock Element

PAUL E. KROEGER, KEVIN D. SARGE, AND RICHARD I. MORIMOTO*

Department of Biochemistry, Molecular Biology and Cell Biology, Northwestern University, Evanston, Illinois 60208-3500

Received 16 December 1992/Returned for modification 9 February 1993/Accepted 18 March 1993

To understand the function of multiple heat shock transcription factors in higher eukaryotes, we have characterized the interaction of recombinant mouse heat shock transcription factors 1 and 2 (mHSF1 and mHSF2) with their binding site, the heat shock element (HSE). For our analysis, we utilized the human HSP70 HSE, which consists of three perfect 5′-nGAAn-3′ sites (1, 3, and 4) and two imperfect sites (2 and 5) arranged as tandem inverted repeats. Recombinant mHSF1 and mHSF2, which exist as trimers in solution, both bound specifically to this HSE and stimulated transcription of a human HSP70-CAT construct in vitro. Footprinting analyses revealed differential binding of mHSF1 and mHSF2 to the HSP70 HSE. Specifically, mHSF1 bound all five pentameric sites, whereas mHSF2 failed to interact with the first site of the HSE but bound to sites 2 to 5. Missing-nucleoside analysis demonstrated that the third and fourth nGAAn sites were essential for mHSF1 and mHSF2 binding. The binding of the initial mHSF1 trimer to the HSE exhibited preference for sites 3, 4, and 5, and then binding of a second trimer occurred at sites 1 and 2. These results suggest that HSF may recognize its binding site through the dyad symmetry of sites 3 and 4 but requires an adjacent site for stable interaction. Our data demonstrate that mHSF1 and mHSF2 bind specifically to the HSE through major groove interactions. Methidiumpropyl-EDTA footprinting revealed structural differences in the first and third repeats of the HSE, suggesting that the DNA is distorted in this region. The possibility that the HSE region is naturally distorted may assist in understanding how a trimer of HSF can bind to what is essentially an inverted repeat binding site.

A well-studied example that has served as a paradigm for activation of gene expression is induction of HSP70 transcription by heat shock transcription factor (HSF). As with other transcription factors, HSF is a member of a family of factors. Smaller eukaryotes (e.g., *Drosophila melanogaster* and *Saccharomyces cerevisiae*) appear at present to have only a single HSF (6, 16, 50) that mediates that response to stressful conditions, whereas larger eukaryotes (e.g., mouse, human, tomato, and chicken) contain multiple HSFs (28, 33, 37, 39, 40). The presence of a family of HSFs suggests that their functions are not redundant and that they act under different or overlapping circumstances. Consistent with this idea, a comparative analysis of the various HSF family members has demonstrated considerable sequence divergence outside the DNA binding and oligomerization domains (28). The cDNAs for two distinct HSFs from mouse have been cloned and sequenced (37). Mouse heat shock factor 1 (mHSF1) and mHSF2 exhibit only 38% identity overall, the homology being primarily due to the high degree of conservation in the DNA binding and oligomerization domains (37). However, between homologs there is significant conservation; for example, mHSF1 and mHSF2 are highly related (>85%) to their respective counterparts in human and avian cells (28, 37).

The DNA-binding ability of HSF1 and HSF2 is latent in vivo (21, 27, 44). And while both HSF1 and HSF2 activate the same target, the HSP70 gene, they respond to distinct stimuli (37, 42). HSF1 DNA binding can be activated in many cell types by stress (heat, heavy metals, and amino acid analogs), whereas HSF2 is unresponsive to these events but is activated when K562 erythroleukemia cells are stimulated to differentiate with hemin. The activation of HSF DNA binding results in the induction of the HSP70 gene, although heat-induced HSF1 and hemin-induced HSF2 do not activate transcription to the same level (42).

Little is known about the functional domains of HSF except the location of the DNA-binding and oligomerization domains (6, 29, 43, 50). The DNA-binding domain of HSFs is localized to the amino terminus of the protein and does not resemble any known DNA-binding motif (6, 28, 33, 37, 40, 50). HSFs are trimeric in structure (32, 36, 45) and appear to oligomerize through heptad repeats into a triple-stranded α-helical coiled coil (32, 45). Human and *Drosophila* HSF has been shown to activate transcription in vitro dependent on the presence of the HSE (6, 33, 40), but the location of HSF activation domains is not well understood.

The heat shock element (HSE), which is the DNA-binding site for HSF, is found in the promoters of stress-responsive genes and is composed of multiple inverted arrays of the pentameric consensus sequence 5′-nGAAn-3′ (2, 31). As with the binding sites of many transcription factors, the HSE has inherent dyad symmetry. Comparison of the HSEs of various organisms reveals that yeast and *Drosophila* HSEs are composed primarily of consensus pentameric sites (5′-nGAAn-3′) (2, 55), whereas in larger eukaryotes only the G residue remains highly conserved, and there are variant sequences, for example, nGGGn and nGACn in the HSP70 HSE that are also contacted by HSF (1, 7, 10).

The analysis of *Drosophila* HSF binding to the HSE demonstrated that HSF interacted with the sequence 5′-nGAAn-3′ when at least two head-to-head or tail-to-tail

* Corresponding author.

repeats were present (31). While *Drosophila* HSF was capable of binding to two sites, the stability increased significantly when three nGAAn sites were present, consistent with the trimeric nature of the protein. Additional studies with three to nine repeats of the basic motif conclusively demonstrated strong cooperativity in the binding of *Drosophila* HSF, such that binding to one trimeric repeat positively influenced and stabilized the binding at adjacent sites (31, 41, 56).

The HSE of the human HSP70 gene contains five nGAAn sites of which sites 1, 3, and 4 match the consensus. Previous characterization of human HSF1 interaction with the human HSP70 HSE in vivo demonstrated that all five consensus G residues were protected from dimethyl sulfate (DMS) methylation by heat shock-activated HSF1 (1). In contrast to HSF1, hemin-activated human HSF2 bound specifically to the HSP70 HSE but failed to substantially protect the consensus G in the first site from DMS methylation (42). In vivo DMS protection studies have consistently shown that the level of methylation protection by human HSF1 is strongest in sites 3 and 4 of the human HSP70 HSE (1), and notably, sites 3 and 4 are consensus nGAAn sites that form a perfect 10-bp dyad symmetry.

We have utilized the human HSP70 promoter for the study of the mHSFs because there is extensive information available regarding the function of this promoter (11, 12, 23, 26, 51–53) and it is the only binding site for which we have an in vivo comparison for HSF1 and HSF2 (42). It should be noted that the human and mouse promoters are 85% identical and that all the basal elements are conserved (15). More importantly, the mouse and human HSEs are both composed of five inverted pentamers, and the first, third, and fourth repeats in each HSE are perfect matches to the consensus.

In this report we have examined the DNA-binding properties of recombinant mHSF1 and mHSF2 to the HSP70 HSE by several different approaches. Although both HSFs share many properties, there are distinct differences in their interactions with the HSE, and these may be related to their distinct roles in vivo as transcriptional activators of heat shock gene expression under differing cellular conditions.

METHODS AND MATERIALS

Overexpression and partial purification of mHSF1 and mHSF2. mHSF1 and mHSF2 were overexpressed in the T7 expression system in the PET3a vector as described by Studier and others (34, 36, 46). Upon lysis of the induced cells, mHSF1 was found in the soluble supernatant, whereas mHSF2 was largely insoluble and found primarily in the pelleted fraction.

The mHSF1 supernatant (from 500 ml of cells) was brought to 100 mM KCl, 12.5 mM MgCl, 10% glycerol, 1 mM phenylmethylsulfonyl fluoride, and 1 mM dithiothreitol (DTT). This fraction was chromatographed on a 20-ml DEAE-Sepharose column with a Pharmacia fast protein liquid chromatography system. The bound mHSF1 was eluted in TM buffer (50 mM Tris-HCl [pH 7.9], 12.5 mM $MgCl_2$, 1 mM DTT, 10% glycerol) at a concentration of ≈0.2 to 0.25 M KCl with a linear gradient from 0.1 to 0.6 M KCl. The pooled fractions were diluted to 0.1 M KCl with TM buffer and chromatographed on a 15-ml heparin-Sepharose column. The bound protein was eluted with a 0.1 to 0.6 M KCl gradient in TM buffer. This step resulted in substantial purification as a majority of the proteins flowed through the column and mHSF1 eluted at ≈0.3 to 0.35 M KCl. This fraction was concentrated and then chromatographed through a Superose 6 sizing column. HSF1 eluted near the void volume of the column. While not homogeneous at this step, HSF1 accounted for >90% of the protein in this fraction.

The purification of mHSF2 was accomplished by resuspending the insoluble mHSF2 pellet from the high-speed centrifugation step in lysis buffer (50 mM Tris [pH 8.0], 2 mM EDTA) and washing the pellet in the same buffer twice. The pellet was resuspended in lysis buffer, and Sarkosyl was added to a final concentration of 1%. Sarkosyl has been previously used to successfully solubilize recombinant actin inclusion bodies (9). This solution was incubated at 25°C for 1 h and then diluted 10-fold with lysis buffer and centrifuged again (30 min, 15,000 × *g*). The supernatant now contained 80% of the mHSF2, and this remained soluble. The supernatant was adjusted to 0.1 M KCl and other components as described above and chromatographed on the heparin-Sepharose column. mHSF2 eluted at 0.3 to 0.35 M KCl, as found earlier for mHSF1.

Plasmid DNAs and the preparation of labeled probes. The plasmids used in transcription studies were LSWT, a human HSP70 promoter construct that contains sequences from −188 to +150 bp of the human promoter linked to the chloramphenicol acetyltransferase (CAT) gene (52). The GRP78-CAT construct was a gift of L. Sistonen in our laboratory and contains 360 bp of the human GRP78 promoter fused to the CAT gene in the pCAT-Basic vector (Promega, Madison, Wis.).

To prepare single-end-labeled probes for footprinting studies, an *Sph*I fragment of the human HSP70 gene promoter from the construct pΔ3 (52) was subcloned into the *Sph*I site of pGEM3. This fragment contains HSP70 promoter sequences from −188 to −4 bp. To label the DNA, we used polylinker sites located at either end of pKΔ3, the *Sal*I site (−188 bp), and the *Hin*dIII site (−4 bp). For mapping mHSF1 and mHSF2 interactions with the HSP70 HSE, we end labeled 5 μg of plasmid DNA at either the *Sal*I or *Hin*dIII site with T4 DNA kinase or *Escherichia coli* Klenow fragment as described previously and digested with the complementary enzyme (35). This resulted in DNA labeled on the coding or noncoding strand at the same end of the molecule. Probes labeled at the *Sal*I site are designated **Sal*I-*Hin*dIII, whereas probes labeled at the *Hin*dIII site are designated *Sal*I-*Hin*dIII*, and the strand (coding or noncoding) is denoted in the legends. The fragments were purified and eluted as described previously (25). The eluted DNA was concentrated by ethanol precipitation and resuspended in 100 μl of 10 mM Tris-HCl (pH 8.0)–1 mM EDTA (TE). Typically, 1 μl (5 to 10 fmol) of DNA (10,000 to 20,000 cpm) was used for footprinting studies. Purine ladders for markers were prepared as described previously (25).

Enzymatic and chemical footprinting. DNase I footprinting was performed as described by Dynan (8). Labeled probe (1 μl), competitor DNA (0.5 μg) poly(dI-dC) · poly(dI-dC), 12.5 μl of 2× transcription buffer (24 mM *N*-2-hydroxyethylpiperazine-*N*′-2-ethanesulfonic acid [HEPES; pH 7.9], 120 mM KCl, 24% glycerol, 16 mM $MgCl_2$, 2 mM DTT, 1 mM EDTA), and mHSF1 or mHSF2 protein (amounts are detailed in the legends to each figure) were added together and brought to 25 μl with water. Incubation was at 23°C for 20 min. The DNase I digestion (2 μg/ml) and gel electrophoresis conditions were as previously described (8). The gel was dried and exposed to XAR-5 film with an intensifying screen at −70°C.

Methidiumpropyl-EDTA (MPE) footprinting was done as described by Hertzberg and Dervan (14) and O'Halloran et

al. (30). The MPE (2.5 μl of a 1.5 mM solution), synthesized by Peter Dervan, was mixed with 4 μl of 4 mM ferrous ammonium sulfate [Fe(II)] and immediately diluted to 100 μl with cold H_2O. One microliter of MPE-Fe(II) was added to the HSF binding reaction. After 3 min, 1 μl of 100 mM DTT was added, and the cleavage reaction was allowed to proceed for an additional 2 min. The reaction was quenched and evaluated as described previously (30).

DMS protection analysis was performed exactly as described previously by O'Halloran et al. (30). After separation of bound and free probe on a native 4% polyacrylamide gel, the bands were electroeluted to NA45 paper (Schleicher & Schuell, Keene, N.H.). The eluted DNA was treated with acid and cleaved with NaOH exactly as previously described (24). The cleavage products were separated on a sequencing gel and visualized by autoradiography.

Missing nucleoside analysis. The conditions used for the assay were essentially as described by Hayes and Tullius (13). Randomly gapped DNA was made with the Fe-EDTA cleavage reaction as previously described (13). Ten-fold scaled-up binding reactions were prepared as for footprinting, and 4 μg of mHSF1 or mHSF2 was added. After 20 min on ice, the bound and free probes were separated by gel shift analysis. The bound and free probes were eluted by crushing and soaking as previously described (25). The eluted DNA was subjected to electrophoresis as described above and analyzed by autoradiography.

Gel shift analysis. Analysis of mHSF1 and mHSF2 binding to end-labeled HSE oligonucleotide probes was done essentially as described previously (27) except that the buffer for the gel was 0.25× TBE. Binding reactions were prepared as described for DNase I footprinting with a double-stranded HSE oligonucleotide comprising all five sites of the human HSE (5′-GGAGGCGAAACCCCTGGAATATTCCCGACC TGGCA-3′). After incubation at 25°C for 20 min, an amount of time sufficient to reach equilibrium, the reactions were loaded on a 4% (40:1) acrylamide gel and subjected to electrophoresis at 150 V for 2 to 3 h. Saturating binding analysis was done similarly, except that the concentration of the DNA was varied from 0.08 to 40 nM and the concentration of the protein was kept constant (30 and 40 ng per reaction for mHSF1 and mHSF2, respectively). Gels were dried and exposed to XAR-5 film with an intensifying screen. The amount of bound and free DNA in the saturating binding analysis was quantitated with the Molecular Dynamics Phosphorimager. The K_d for mHSF1 and mHSF2 was determined from Scatchard analysis and the equation of the best-fit line with the formula $K_d = -1/\text{slope}$.

Chemical cross-linking. Analysis of HSF oligomerization by ethylene gylcol-bis(succinimidylsuccinate) (EGS) cross-linking was done exactly as described previously, and the cross-linked products were visualized by Western blot (immunoblot) analysis with antisera specific for mHSF1 or mHSF2 (6, 36).

Transcription assays. Reaction mixtures were prepared on the basis of published methods (3, 18, 26). Components were assembled in microcentrifuge tubes on ice as follows: 12.5 μl of 2× transcription buffer, 250 ng of template DNA (LSWT and GRP78-CAT), 20 μg of concentrated (10-mg/ml) HeLa cell nuclear extract prepared as described previously (8, 26), and various amounts of mHSF1 and mHSF2. Reaction mixtures were allowed to equilibrate on ice for 5 min, and then 5 μl of a 7 mM solution of all four ribonucleoside triphosphates (ATP, GTP, CTP, and UTP) was added and the reaction mixture was placed at 37°C for 90 min. The reaction was quenched with 100 μl of stop buffer (1× stop buffer is 20 mM EDTA, 200 mM NaCl, and 250 μg of tRNA). Two phenol-chloroform extractions were performed, and the nucleic acids were precipitated. After centrifugation (15 min, 12,000 × *g*), the pellets were washed with 80% ethanol and resuspended in 16 μl of TE and 4 μl of 5× hybridization buffer (1.25 m KCl, 10 mM Tris-HCl [pH 7.9], 1 mM EDTA). Nine microliters of the RNA was removed to a new tube, mixed with 1 μl of end-labeled CAT primer (50 fmol), denatured at 85°C for 5 min, and hybridized for 20 min at 56°C. The primer was complementary to a 24-nucleotide (nt) region of the CAT coding sequence (from nt +26 to +49 of the CAT coding sequence). The hybridization was placed on ice and diluted with 23 μl of primer extension buffer (1× primer extension buffer is 20 mM Tris-HCl [pH 8.0 {at 23°C}], 10 mM $MgCl_2$, 5 mM DTT, 10 μg of actinomycin D per ml, and 0.5 mM [each] deoxynucleoside triphosphate). The reaction mixtures were warmed to 42°C, and 50 U of mouse mammary leukemia virus reverse transcriptase (Bethesda Research Laboratories, Bethesda, Md.) was added. After 1 h, the reaction mixture was precipitated with ethanol, centrifuged (15 min, 12,000 × *g*), and resuspended in sample buffer and electrophoresed on a denaturing acrylamide gel. The gel was dried and exposed to film with an intensifying screen. Reverse transcription of the CAT primer to the start of transcription results in a 236- and 130-nt product for the HSP70 and GRP78 constructs, respectively. Quantitation of radioactive signals was performed on the Molecular Dynamics Phosphorimager as described by the manufacturer.

RESULTS

Characterization of the oligomeric state of mHSF1 and mHSF2. To examine the biochemical properties of mHSF1 and mHSF2, the genes encoding both proteins were inserted into T7 overexpression vectors and the corresponding proteins were purified as described in Materials and Methods. Two micrograms of mHSF1 after the Superose 6 column (Fig. 1A, lane B) and mHSF2 after the heparin column (Fig. 1A, lane C) was loaded on a sodium dodecyl sulfate (SDS)–10% polyacrylamide gel, and the protein bands were subsequently visualized by Coomassie brilliant blue staining. By this analysis, recombinant mHSF1 and mHSF2 have apparent molecular masses of 67 and 70 kDa, respectively. mHSF1 and mHSF2 represented greater than 90% of the protein in these fractions. The band above mHSF1 comigrates through three columns; however, it is not antigenically related to mHSF1, as determined by Western blot analysis with antisera specific to mHSF1 (data not shown). The additional bands in the gel below the 70-kDa mHSF2 are all antigenically related to mHSF2 and most likely represent degradation products.

Yeast HSF has been reported to be a trimer (45), whereas activated *Drosophila* HSF has been reported to be a trimer (31) and a hexamer (49). Our laboratory has shown that HSF1 in vivo is in an inactive state and primarily monomeric and upon activation becomes trimeric (36). In vivo, HSF2 is primarily dimeric and upon activation by hemin acquires a native size consistent with a trimer (36, 41a). The fact that the HSFs are synthesized as active DNA-binding proteins in bacteria but are expressed in a non-DNA-binding form in eukaryotic cells suggests that they are under negative regulation. Curiously, if the proteins are synthesized in vitro in reticulocyte lysates, HSF1 DNA binding is heat inducible but HSF2 binding is constitutive (37). Thus, it appears that

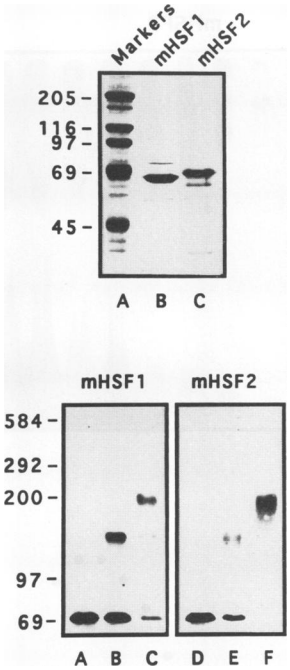

FIG. 1. Protein analysis and determination of oligomeric structure. (A) Two micrograms of purified mHSF1 and mHSF2 was subjected to electrophoresis in an SDS–10% polyacrylamide gel and stained with Coomassie blue. Lane A, molecular mass markers: myosin (205 kDa), β-galactosidase (116 kDa), phosphorylase B (97 kDa), bovine serum albumin (69 kDa), and ovalbumin (45 kDa); lane B, mHSF1; lane C, mHSF2. (B) EGS cross-linking of mHSF1 (lanes A to C) and mHSF2 (lanes D to F). Lanes: A and D, un-cross-linked controls; B, 0.05 mM EGS; C, 0.2 mM EGS; E, 0.2 mM EGS; F, 1.0 mM EGS. Molecular mass markers are bovine serum albumin (69 kDa) and cross-linked multimers of phosphorylase B (97, 200, 292, and 584 kDa).

the environment in which the HSF is synthesized determines it activation state.

In order to establish the native complex size of the purified recombinant mHSF1 and mHSF2, both proteins were subjected to cross-linking with the chemical reagent EGS and the cross-linked products were detected by Western blot analysis with antisera specific to mHSF1 and mHSF2. At a protein concentration (40 ng/ml [36]) that mimicked the in vivo concentration of HSF1 and HSF2, the results show that both mHSF1 and mHSF2 exist predominantly as trimers in solution. Figure 1B demonstrates that as the concentration of EGS was increased from 0.05 to 0.2 mM for mHSF1 and 0.2 to 1.0 mM for mHSF2, the largest cross-linked product detectable was consistent with the size of a trimer for both mHSF1 (lane C, 210 kDa) and mHSF2 (lane F, 210 kDa). mHSF2 required higher levels of EGS for efficient cross-linking; however, this is likely due to the inherent differences in the protein sequences of mHSF1 and mHSF2. These results show that purified recombinant mHSF1 and mHSF2 proteins are both trimers in solution and are consistent with the conservation of the oligomerization domains and previous analysis of other HSFs (31, 32, 36, 37, 45).

Determination of apparent dissociation constants for mHSF1 and mHSF2. The existence of multiple HSFs and their differential regulation has raised questions regarding their DNA-binding properties. Do all HSFs have the same affinity for their binding site? To address this question, saturation binding was performed (5, 38) to determine the apparent dissociation constants (K_d) for recombinant mHSF1 and mHSF2. A constant amount of mHSF1 or mHSF2 was incubated with various concentrations of HSE probe, and the K_d values were calculated by Scatchard analysis. After gel shift analysis (Fig. 2A and B, top panels) the amount of bound and free probe was quantitated with a Molecular Dynamics Phosphorimager. The results were graphed to demonstrate saturation (bound versus total [middle panels]) or analyzed by the method of Scatchard (bottom panels, Bound/Free versus Bound) to determine the K_d (5, 38). We note that both binding isotherms (Fig. 2A and B, middle panels) are sigmoidal in shape, and this is consistent with the cooperative nature of HSF binding to DNA that has been described previously (31, 56). We chose to measure the K_d by quantitating the entire shifted set of DNA-protein complexes. For comparative purposes, we plotted a linear line of best fit through the datum points (Fig. 2A and B, bottom panels) and determined that mHSF1 and mHSF2 had nearly identical K_d values of 2.7 and 2.4 nM, respectively.

Activation of transcription by mHSF1 and mHSF2. In order to directly compare their transcriptional activities, purified mHSF1 and mHSF2 were added to an in vitro transcription system by using DNA templates corresponding to the human HSP70 promoter (LSWT) and a control promoter lacking HSEs, the GRP78/Bip promoter (GRP78-CAT). Purified mHSF1 (Fig. 3, lanes D and E) or mHSF2 (lanes F and G) (150 ng) was added to duplicate reaction mixtures. The reaction mixtures were incubated and processed as described in Materials and Methods, and the levels of HSP70 and GRP78 transcription were assayed by primer extension. Both HSF factors positively stimulated transcription from the HSP70 promoter relative to control reactions (lanes B and C), in which no HSF was added. In numerous assays, mHSF1 stimulated basal transcription 3- to 4-fold (lanes D and E), whereas mHSF2 (lanes F and G) stimulated transcription only an average of 1.5- to 2-fold. The addition of mHSF1 or mHSF2 lowered the level of transcription from the GRP78-CAT construct present in the same reaction by 10 to 20%. The level of transcriptional activation by mHSF1 and mHSF2 in vitro was dependent on protein concentration as the level of measurable RNA increased linearly with the addition of up to 75 ng of mHSF1 protein per assay (data not shown). Addition of more protein gave relatively little increase in the level of transcription, so 150 ng of protein was routinely used per assay for our experiments. This amount of mHSF1 or mHSF2 represents approximately a 10-fold excess of trimeric HSF over available HSE binding sites in the reaction (5-fold if two trimers bind).

Analysis of mHSF1 and mHSF2 protein-DNA interactions with enzymatic and chemical footprinting. Since it appeared that mHSF1 and mHSF2 had similar affinity for the HSE and that their oligomeric state was essentially identical, it was important to know whether the differences we observed in transcriptional activation in vivo and in vitro reflected differences in the interaction of mHSF1 and mHSF2 with the HSE. To address this question, we utilized several complementary approaches to examine mHSF1 and mHSF2 interaction with the HSE. These included DNase I footprinting, hydroxyl radical footprinting, DMS protection, and missing nucleoside analysis. Each method, as detailed below, offers a different view of the HSF-HSE interaction.

DNase I footprinting. This method can provide information about the location of protein-DNA interaction and the approximate boundaries of interaction along the phosphate backbone of the DNA. Initial binding analyses, as measured

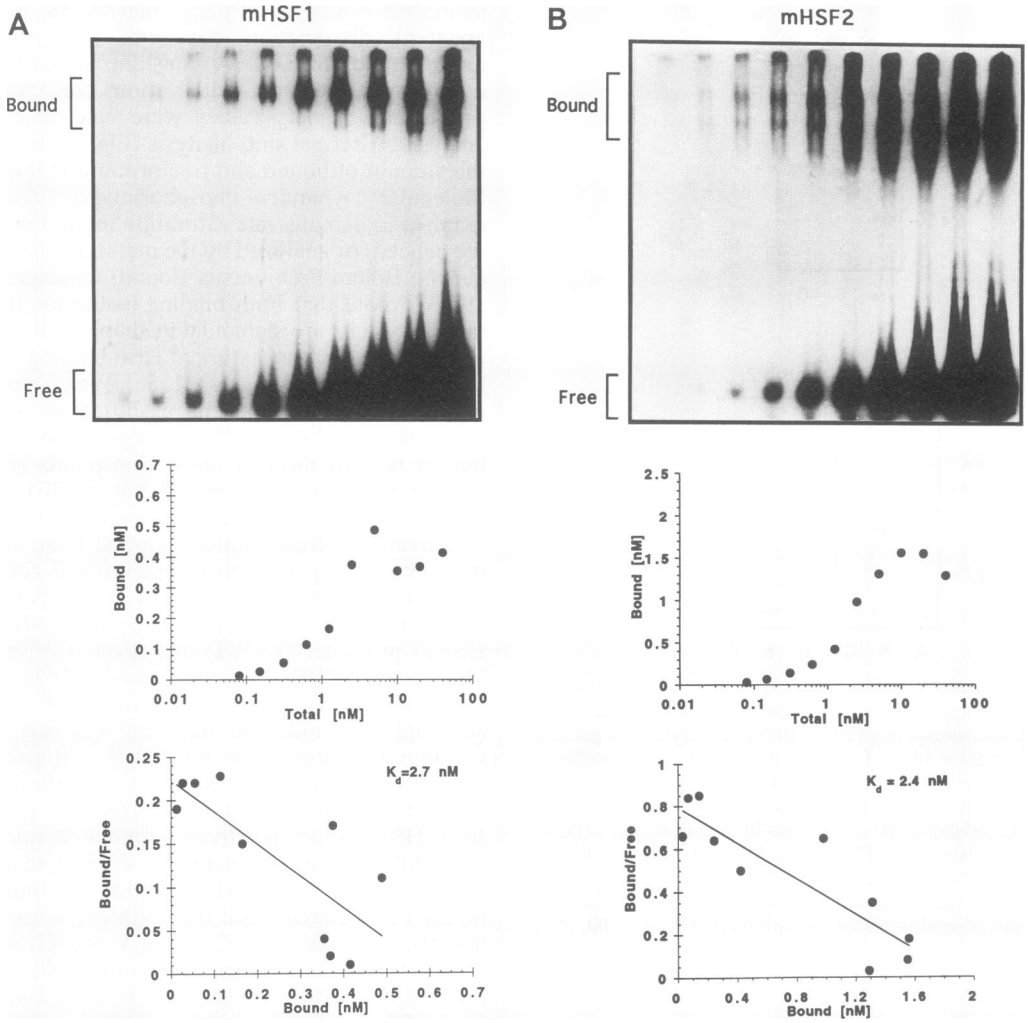

FIG. 2. Apparent dissociation constant determination for mHSF1 and mHSF2. Saturation binding was performed as described in Materials and Methods. The concentration of the protein was kept constant, and the amount of labeled probe was varied from 0.08 to 40 nM. The apparent K_d was calculated from the slope of the best-fit line for the Scatchard plot. Upper panels, gel shift analysis of mHSF1 and mHSF2 binding. Middle panels, plot of bound DNA versus total DNA. Bottom panels, Scatchard analysis of binding data graphed as bound/free versus bound. The equation for the line of best fit in the mHSF1 Scatchard plot is $y = 0.22362 + -0.36931x$ and $R = 0.77792$. The equation for the line in the mHSF2 plot is $y = 0.79368 + -0.41581x$ and $R = 0.8787$. The K_d values for mHSF1 and mHSF2 are inset in the bottom panels.

by gel shift analysis, demonstrated that our preparations of mHSF1 and mHSF2 were nearly identical in binding activity (data not shown). We established binding reactions as described in Materials and Methods with **SalI-HindIII* DNA probes and, after DNase I digestion, analyzed the products on denaturing sequencing gels (Fig. 4A and B). Partial protection of the entire HSE, from nucleotides −119 to −86 (coding strand) and −120 to −86 (noncoding strand) was detected at low concentrations of mHSF1 (37.5 ng or 9 nM) (Fig. 4A, lane C, and 4B, lane B). As the level of mHSF1 protein increased, the coding (Fig. 4A, lanes D to F) and noncoding (Fig. 4B, lanes C to E) strand footprints became more pronounced. mHSF2 exhibited a similar pattern of protection with increasing protein concentration (Fig. 4A, lanes I to L, and 4B, lanes H to K), and the boundaries of protection were from nt −112 to −86 on the coding strand and nt. −115 to −90 on the noncoding strand. Densitometry was utilized to quantitate the level of protection by mHSF1 and mHSF2 in various regions of the HSE. mHSF1 protection at the lowest concentration (9 nM) was ≈75% throughout the HSE (Fig. 4A, lane C). The protection by mHSF2 was the same, except in the region of site 1, where the level of protection was only 25 to 45% and did not increase significantly with additional protein. The results of the DNase I footprinting analysis are schematically outlined in Fig. 4C. The boundaries of mHSF1 and mHSF2 interaction were measured at the concentration of protein that produced a saturated footprint (300 ng, which corresponds to a 100-fold molar excess of HSF trimer over binding site). Addition of more protein did not change the boundaries of interaction. The extent of protection by mHSF1 is consistent with the presence of a monomer of mHSF1 bound to each site within the HSE. Thus, the mHSF1 and mHSF2 footprints were similar except at the distal boundary, where there was a 5 to 7 nt difference in the extent of protection in site 1. One interpretation of our data is that mHSF1 is bound to sites 1 to 5 of the HSE, whereas mHSF2 fails to interact substantially with site 1 and protects only sites 2 to 5.

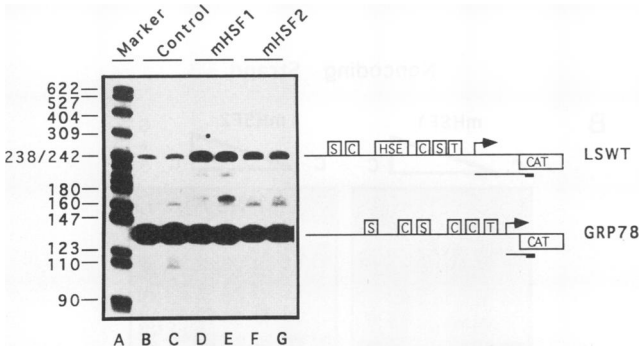

FIG. 3. Transcriptional activation by mHSF1 and mHSF2. Transcription reaction mixtures were prepared as described in Materials and Methods. Lane A, markers prepared from *Hpa*II-digested pBR322 DNA. Sizes of bands are denoted to the left. Lanes B and C, control reactions without added mHSF1 or mHSF2. Lanes D and E and F and G, duplicate reactions with 150 ng of recombinant mHSF1 or mHSF2, respectively. The activation of transcription was measured on LSWT, and the control construct GRP78-CAT was included in all reaction mixtures. The amount of transcriptional stimulation was measured by quantitating the radioactive signals with the Phosphorimager (Molecular Dynamics). The promoters of both constructs are schematically drawn to the right, adjacent to the corresponding band in the autoradiogram. The boxed letters designate the different protein binding sites in each promoter. S, Sp1 site; C, CCAAT box; T, TATA box; HSE, heat shock element. The relative position of the CAT gene to the start of HSP70 or GRP78 transcription (denoted with arrow) is shown. Also, the positions of the CAT primer and the reverse-transcribed product are designated below each schematic.

MPE footprinting. To further analyze the binding of mHSF1 and mHSF2, hydroxyl radical footprinting was performed with MPE (14, 30). MPE is a useful footprinting reagent because it generates DNA cleavage at nucleotide resolution. The MPE reaction produces hydroxyl radicals directly in the minor groove of the DNA by virtue of the intercalative binding of the methidium moiety. The cleavage of DNA by MPE is sensitive to the shape of the minor groove and can therefore also give information on the structure of DNA in the minor groove (48). MPE permits an assessment of the contact points by a protein along the DNA backbone and gives specific information regarding the interaction of protein with the ribose residues. The hydroxyl radical cleavage reagent is small and can therefore penetrate regions of protein-DNA interaction inaccessible to DNase I. This analysis results in an examination of the tightest interactions between the protein and DNA.

Increasing amounts of mHSF1 or mHSF2 were incubated with **Sal*I-*Hin*dIII DNA probes and then treated with MPE as described in Materials and Methods. The sequence protected by mHSF1 was from nt −113 to −91 and −116 to −92 on the coding and noncoding strands, respectively (Fig. 5A, lanes C to E and M to O) and was consistent with results obtained with Fe-EDTA hydroxyl radical footprinting (data not shown). The protection by mHSF2 (lanes G to I and Q to S) was nearly identical to mHSF1 on both strands and the results are summarized in Fig. 5B. Even though there was modulation in the level of cleavage (see below), the level of protection for mHSF1 and mHSF2 in sites 2, 3, and 4 was greater than 90% as judged by densitometry. These results suggest that the tightest interactions of both mHSF1 and mHSF2 are in the phosphate-ribose backbone within sites 2, 3, and 4. The lack of significant protection in sites 1 and 5 is not inconsistant with our DNase I results but suggests that the association of HSF with flanking sites may not be as tight as that found with internal sites.

The MPE footprinting analysis also yielded an unexpected result, in that in the absence of added HSF, two regions in the HSE were minimally cleaved by MPE (Fig. 5A, lanes B and L; Fig. 5B, Control). This modulation of cleavage level through the HSE was also evident in Fe-EDTA footprinting reactions, but to a much lower extent (data not shown). These areas of low MPE cleavage occurred at the end of tracts of adenine residues. Specifically, the minimal MPE cleavage occurred at nt −100 and −111 on the coding strand and nt −101 and −112 on the noncoding strand. As originally demonstrated for the phased A tracts of kinetoplast DNA (4), the regions of minimal cleavage on each strand in the HSE are shifted by 1 base in the 3′ direction. This shift is generated because of the relative positions of the ribose residues in the minor groove and is characteristic of hydroxyl radical cleavage (4). The maximal cleavage between the minima is also offset by 2 bp to the 3′ side. The implications of this lowered reactivity are that the DNA in this region is distorted. The minor groove in the HSE between sites 1 and 2 and sites 3 and 4 is likely narrowed and therefore unavailable for intercalative binding by MPE.

DMS protection analysis. The MPE footprinting confirmed that both proteins made significant contacts with the DNA backbone. However, since MPE generates hydroxyl radicals in the minor groove, we were interested in whether mHSF1 or mHSF2 actually contacted the DNA through minor groove interactions. To address this question, a DMS protection experiment was performed (30) with a modified cleavage reaction to detect both methylated G residues (major groove) and methylated A residues (minor groove) (24). The results of our analysis are shown in Fig. 6. mHSF1 protected the G residues of all five repeats (nt −94, −104, −105, and −114 on the coding strand and nt −97 and −107 on the noncoding strand) and only one A residue in the minor groove at position −106 on the noncoding strand. The level of protection from methylation at all positions was 40 to 50% as judged by densitometry. mHSF2 binding was apparently not as tight, since protection from methylation was detected only at the G residues (−104 and −105) in site 3 and at the same A residue (−106) as seen for mHSF1. There was no protection by mHSF2 at the consensus G residues in sites 1 and 2 (−114 and −110), and the level of protection at the concensus G (−94) in site 5 was 20%. The differences observed here reflect bound protein, because the binding reactions were subjected to gel shift analysis after DMS treatment. It can be concluded that mHSF1 or mHSF2 primarily contact the major groove and that the protection from hydroxyl radical cleavage is the result of HSF interaction with the phosphate-ribose backbone. The protection of the A residue at −106 suggests a minor groove contact, and this has been observed previously in studies of *Drosophila* HSF interaction with the *Drosophila* HSP70 HSE.

There were prominent DMS hypersensitivities induced by mHSF1 at positions G-89 and G-116 on the coding strand and G-95 on the noncoding strand. These same DMS hypersensitivities for HSF1 have been observed before with in vivo methylation experiments in heat-shocked HeLa cells (1, 42) and may reflect structural changes in the HSE upon binding of HSF or the formation of hydrophobic pockets more conducive to DMS methylation. In contrast, mHSF2 binding resulted in DMS hypersensivity only at position G-95, unlike the in vivo results of hemin-induced HSF2 (42), perhaps reflecting the general lack of tight association in vitro.

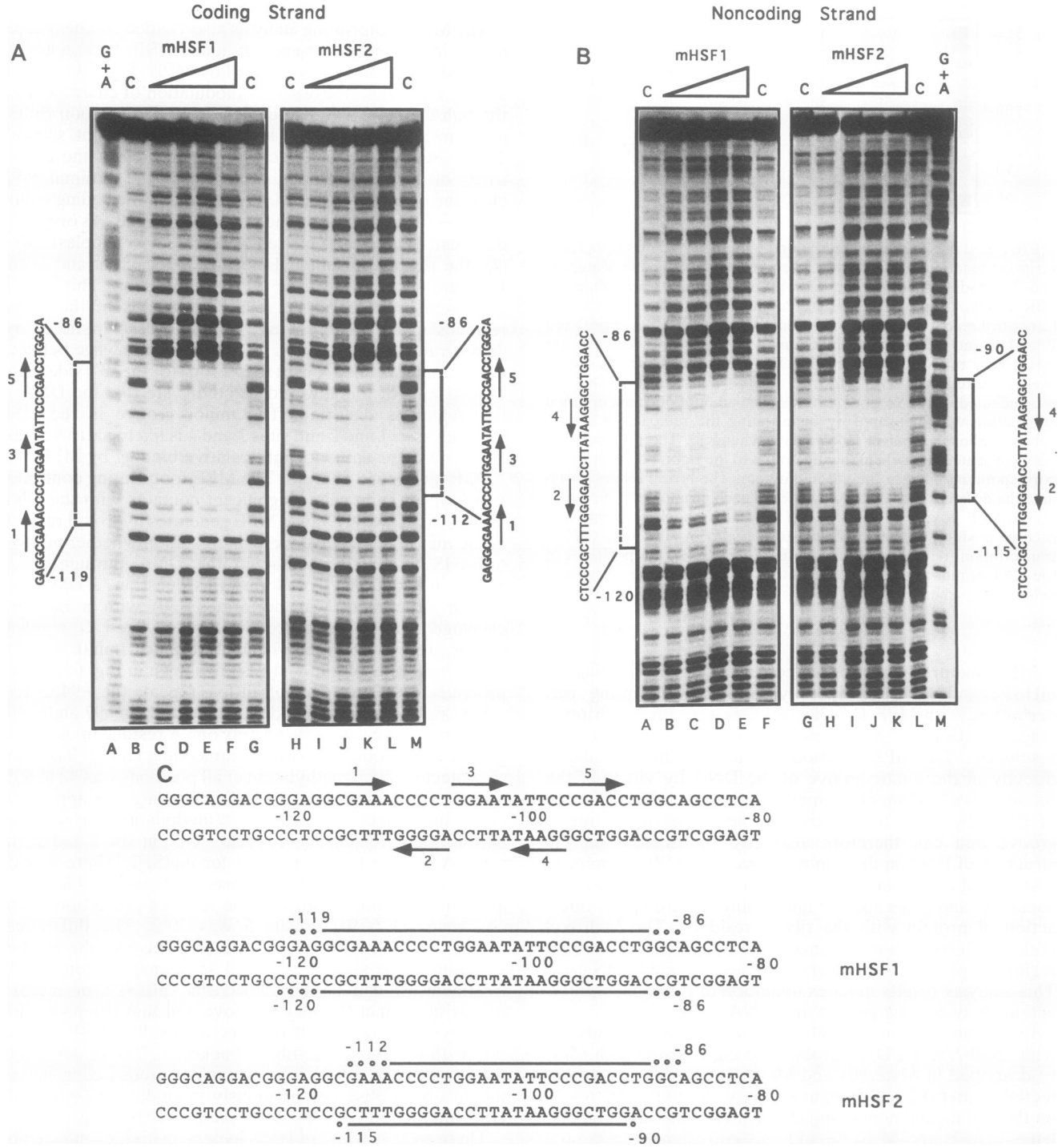

FIG. 4. DNase I footprinting of mHSF1 and mHSF2 binding to the HSP70 HSE. Reaction mixtures were prepared and analyzed as described in Materials and Methods. (A) Coding strand footprints. Lanes: A, G + A ladder of *SalI-HindIII; B, G, H, and M, control DNase I digestions; C to F, increasing concentration of mHSF1 (37.5, 75, 150, and 300 ng); I to L, increasing concentration of mHSF2 (37.5, 75, 150, and 300 ng). (B) Noncoding strand footprints. Same as panel A, except analysis is of the noncoding strand. (C) Summary of DNase I protection data. The sequences of both strands are shown, and the positions of the individual binding sites are denoted with arrows and numbers. The extent of protection on the coding and noncoding strands by mHSF1 and mHSF2 is shown with solid lines above and below. Regions where protection was not complete or the boundary was not exact are denoted with open circles. The numbers adjacent to each footprint (coding and noncoding) designate the nucleotide at which protection stops.

Additionally, it is possible that there was some activated HSF1 in the hemin study that contributed to the hypersensitivity seen in those experiments (42).

Missing-nucleotide analysis of HSF1 and HSF2 binding. The results of the various footprinting analyses revealed that mHSF1 and mHSF2 might differ in their preference for certain repeats of the HSE. To address this, we used the missing-nucleotide technique (13), which permits an assessment of the bases in a binding site that are necessary for stable protein interaction. These experiments also allowed us to understand how an HSF trimer interacts with a five-unit binding site such as the HSP70 HSE. There are three possible arrangements that a trimer of HSF can have on a five-repeat binding site. For example, a trimer of mHSF1 or mHSF2 could bind to sites 1, 2, and 3; 2, 3, and 4; or 3, 4, and 5.

To perform the missing nucleoside analysis, the DNA was first treated with hydroxyl radical to remove a single base from each DNA fragment (Fig. 7A, schematic). The gapped DNA was then used as a substrate for a protein binding reaction under saturating binding conditions. The binding reaction was separated in a gel shift assay, and the bound and unbound DNA were isolated from the gel and run on a denaturing sequencing gel. Examination of the unbound fraction reveals those bases that are essential for binding. In contrast, the bound fraction ideally contains all bases except those found in the unbound fraction and appears as a footprint. The reciprocal nature of this analysis reinforces the interpretation of the result. **Sal*I-*Hin*dIII end-labeled DNA (coding or noncoding strand) was treated with hydroxyl radical, the gapped DNA was purified, and a saturating gel shift was performed with mHSF1 and mHSF2 (Fig. 7B). In the mHSF1 binding reaction, two complexes were detectable with the coding and noncoding strand probes; a minor, faster-migrating complex, labeled A, and a more slowly migrating complex, denoted B (Fig. 7B, lanes A and B).

To determine the bases required for mHSF1 binding, the unbound fraction of the coding and noncoding strands was examined. As shown in Fig. 7C (lanes B and G), there was an enrichment of bases positioned in sites 3 and 4. Specifically, G-104, A-103, A-100, T-99, and T-98 on the coding strand and T-103, T-102, and A-101 on the noncoding strand were most prominent, thus indicating that a loss of any one of these nucleotides leads to an inability to bind stably to mHSF1 (Fig. 7D, schematic). These results suggest to us that mHSF1 prefers to bind to a trimeric repeat and that it may be the dyad symmetry of sites 3 and 4 that are most important in the stable recognition of the HSE by mHSF1 and mHSF2. In support of this hypothesis, we have found in gel shift experiments that a dimeric HSE probe (5′-TCGGA TGGAATATTCCCTAGCT-3′) comprising sites 3 and 4 is bound surprisingly well by mHSF1 and mHSF2, with approximately a two to fourfold-reduced affinity compared with a probe comprised of three sites (3, 4, and 5) (data not shown). HSF binding to a dimeric repeat that is a nonconsensus sequence (5′-AGGGGACTTTCCGA-3′) and not dyad symmetrical is significantly weaker (10- to 20-fold). Additionally, both of these oligonucleotides were ineffective competitors of HSF bound to HSE probes composed of three or more sites. These results suggest that if site 3 is destroyed in the missing-nucleoside analysis, then binding to the remaining dimeric sites (1 and 2 or 4 and 5) is very unfavored. Next, the DNA in the bound complexes was examined to determine the bases that were missing or enhanced in complexes A and B.

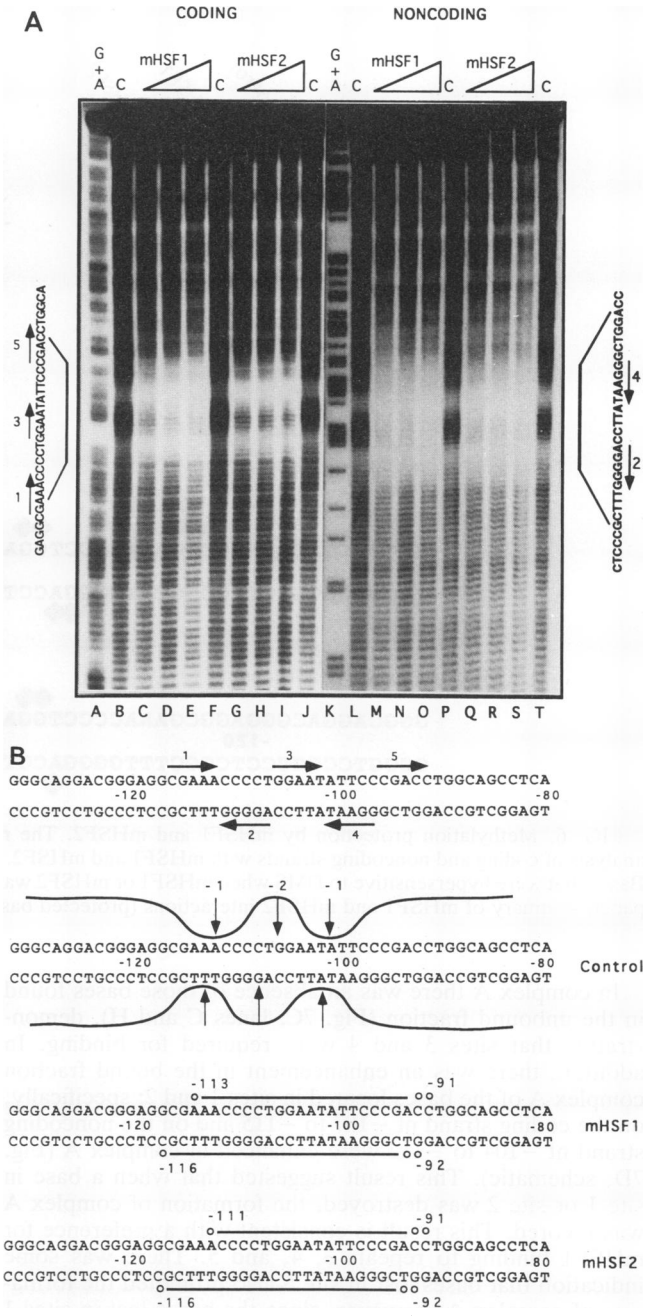

FIG. 5. MPE footprinting. (A) mHSF1 and mHSF2 footprints on the coding and noncoding strands of the HSP70 promoter. Reaction mixtures contained **Sal*I-*Hin*dIII probe DNA labeled on either the coding strand (lanes A to J) or the noncoding strand (lanes K to T) and were performed as stated in the text. The extent of HSE protection was analyzed by laser densitometry. Lanes: A and K, G + A sequencing ladders; B, F, J, L, P, and T, control reactions without added mHSF protein; C to E and M to O, mHSF1 added (300, 600, and 1,200 ng, respectively); G to I and Q to S, mHSF2 added (300, 600, and 1,200 ng, respectively). The extent of protection is denoted at the side with the sequence of the appropriate strand, and the HSE sites are marked. (B) Schematic summary of mHSF1 and mHSF2 MPE footprinting. Protection is denoted with lines and open circles. The control schematic depicts the relative level of MPE cleavage in the HSE region with a line. The depressions in the curve designate the regions of lower MPE cleavage discussed in the text. The numbers denote the amount of 3′ offset (in bases) of the minimal and maximal cleavage regions on both strands at sites 1 and 3.

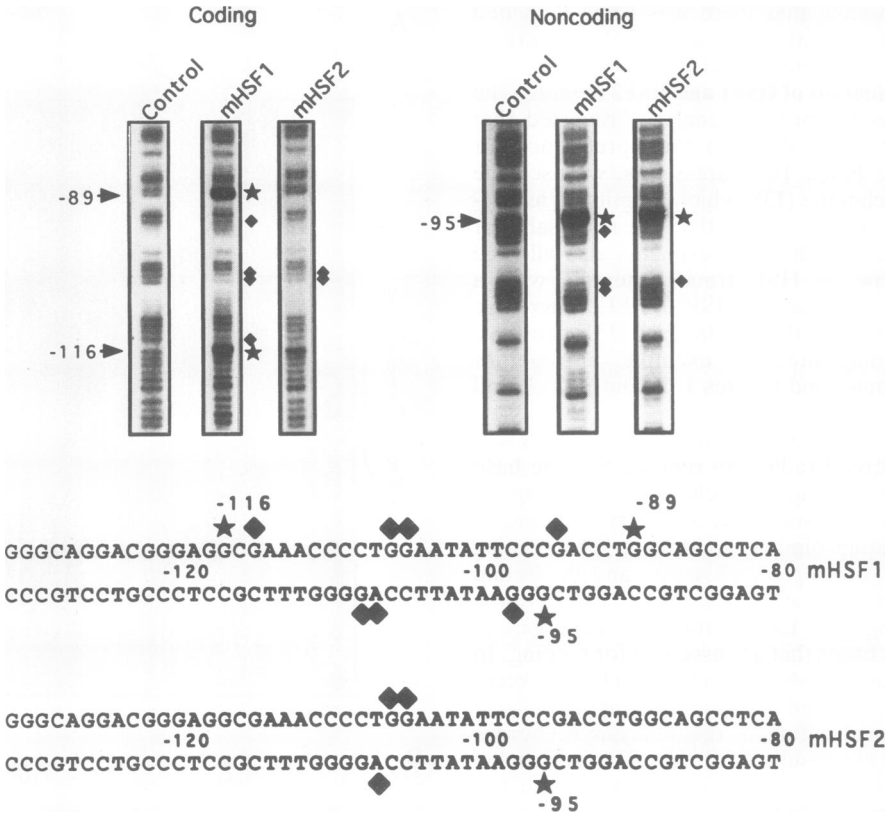

FIG. 6. Methylation protection by mHSF1 and mHSF2. The reactions were as described in the text. Upper panel, DMS protection analysis of coding and noncoding strands with mHSF1 and mHSF2. The bases protected from methylation are denoted with a solid diamond. Bases that were hypersensitive to DMS when mHSF1 or mHSF2 was bound to the HSE are noted with arrows and marked with stars. Bottom panel, summary of mHSF1 and mHSF2 interactions (protected bases and DMS hypersensitivities) in the HSE region.

In complex A there was an absence of those bases found in the unbound fraction (Fig. 7C, lanes C and H), demonstrating that sites 3 and 4 were required for binding. In addition, there was an enhancement in the bound fraction complex A of the bases located in sites 1 and 2; specifically, on the coding strand nt −107 to −115 and on the noncoding strand nt −104 to −112 were enhanced in complex A (Fig. 7D, schematic). This result suggested that when a base in site 1 or site 2 was destroyed, the formation of complex A was favored. This result is consistent with a preference for mHSF1 binding to repeats 3, 4, and 5. There was some indication that bases lost in site 5 also promoted the formation of complex A; however, since the bases lost in sites 1 and 2 were more prominent, we think that the binding of mHSF1 must be more stable when bound to sites 3, 4, and 5. If another combination of binding sites was preferred (e.g., 1, 2, and 3 or 2, 3, and 4), then cleavage at the corresponding bases should have been enhanced in complex A.

Examination of the bases missing from mHSF1 complex B demonstrated a definite footprint area, especially on the noncoding strand (Fig. 7C, lanes D and I). Consistent with our hypothesis regarding the requirement for a trimeric binding site, it was found that the bases in site 3 were the weakest in intensity in complex B (lanes D and I). Specifically, on the coding strand G-104, A-100, T-99, and T-98 and on the noncoding strand T-103, T-102, and A-101 were absent in complex B. The missing-nucleoside footprint for mHSF1 binding in complex B encompassed sites 1 to 4, the

FIG. 7. Missing-nucleoside analysis of mHSF1 and mHSF2 binding. (A) Summary of the missing-nucleoside experiment protocol. a, production of randomly gapped DNA (hypothetical HSE fragment) by treatment with hydroxyl radical; b, binding of HSF to gapped DNA; c, separation of bound and free probe DNA. Only one strand is labeled, denoted by the asterisk. Single nucleotides are removed from each fragment, and HSF can bind to all fragments except those that lost an essential base. (B) Preparative gel shift of mHSF1 and mHSF2 with gapped coding and noncoding strand probes (*SalI-HindIII). The location of free probe (F) and complexes A and B are noted at the left. (C) Missing-nucleoside analysis of mHSF1. Lanes, A to E, coding strand; F to J, noncoding strand; A and F, G + A ladder; B and G, unbound probe; C and H, mHSF1 bound complex A; D and I, bound complex B; E and J, probe DNA control. The sequence of the HSE region on both strands is depicted, and the positions of the binding sites are marked. (D) Summary of mHSF1 missing-nucleoside data. In the unbound schematic (top), the height of the black bar indicates the intensity of the base found in the unbound fraction. In complex A (middle), the open squares denote bases that, when lost, accentuated the formation of complex A. The filled circles denote bases missing in mHSF1 complex A. In complex B (bottom), the bars denote the footprint area, and the filled circles denote the bases missing from the complex B fraction. (E) Missing-nucleoside analysis of mHSF2. Lanes A to D, coding; E to H, noncoding; A and E, G + A ladder; B and F, unbound DNA; C and G, bound complex B; D and H, probe DNA control. (F) Summary of mHSF2 missing-nucleoside data. The designations are the same as in panel D.

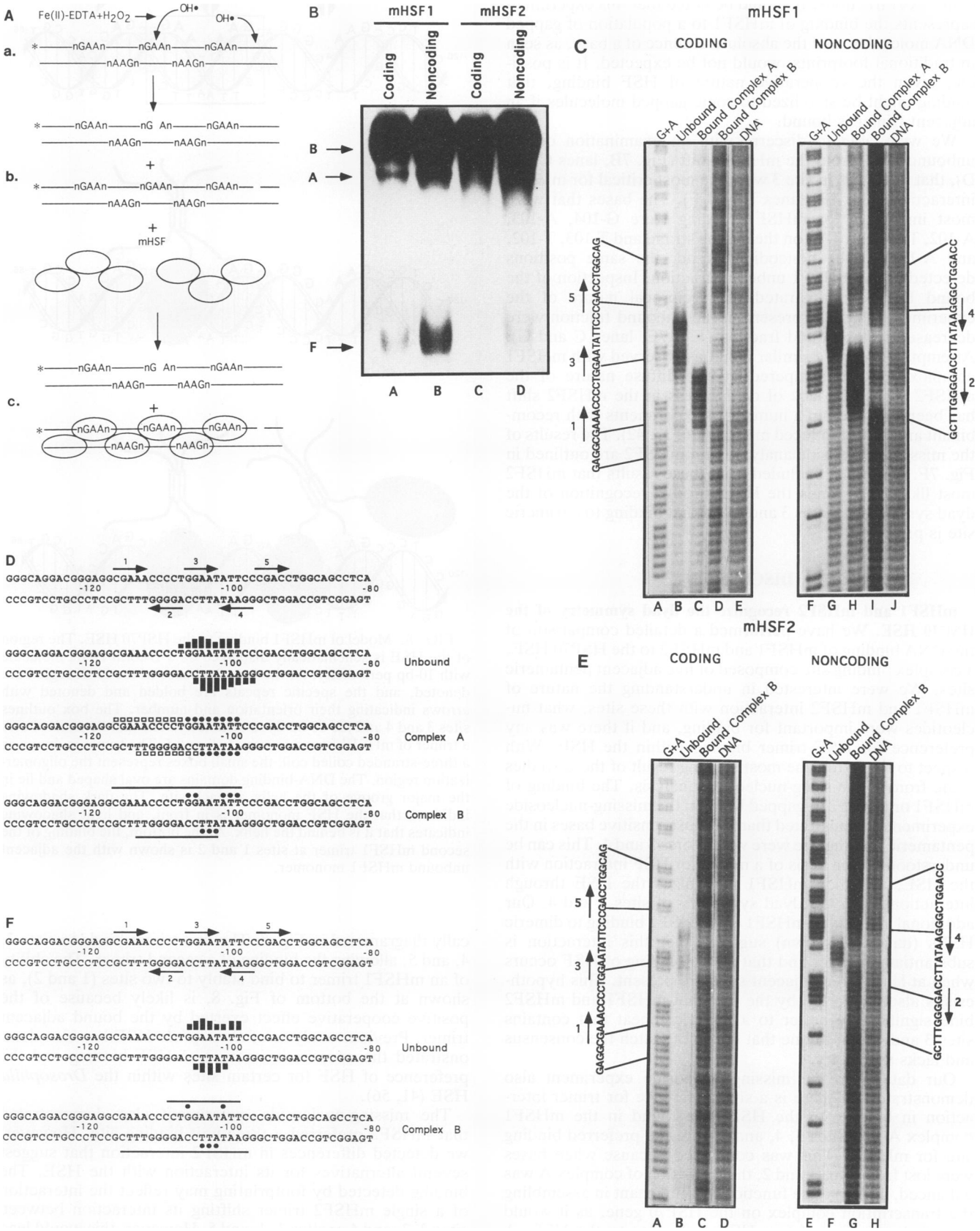
A
Fe(II)-EDTA+H2O2
OH•
a.
b.
c.
mHSF
nGAAn
nAAGn
B
mHSF1
mHSF2
Coding
Noncoding
B
A
F
A B C D
C
mHSF1
CODING
NONCODING
G+A
Unbound
Bound Complex A
Bound Complex B
DNA
A B C D E
F G H I J
mHSF2
D
GGGCAGGACGGGAGGCGAAACCCCTGGAATATTCCCGACCTGGCAGCCTCA
CCCGTCCTGCCCTCCGCTTTGGGGACCTTATAAGGGCTGGACCGTCGGAGT
Unbound
Complex A
Complex B
E
A B C D
E F G H

region where sensitive bases were found in the unbound or complex A fractions. It should be noted that this experiment represents the binding of mHSF1 to a population of gapped DNA molecules, and the absolute absence of a base, as seen in traditional footprints, would not be expected. It is possible, given the cooperative nature of HSF binding, that binding might be stabilized to some gapped molecules if an adjacent trimer is bound.

We were able to discern, with an examination of the unbound DNA from the mHSF2 shift (Fig. 7B, lanes C and D), that the bases in site 3 were the most critical for mHSF2 interaction (Fig. 7E, lanes B and F). The bases that were most important for mHSF2 binding were G-104, A-103, A-102, T-99, and T-98 on the coding strand and T-103, T-102, and A-101 on the noncoding strand, the same positions detected in the mHSF1 unbound fraction. Inspection of the bound DNA demonstrated the reciprocal nature of the experiment, as bases present in the unbound fraction were decreased in the bound fraction (Fig. 7E, lanes C and G). Attempts to detect a similar result as observed with mHSF1 complex A were hampered by the diffuse nature of the mHSF2 shift. The lack of distinctness in the mHSF2 shift has been observed in a number of experiments with recombinant and hemin-induced mHSF2 (36, 37, 42). The results of the missing-nucleoside analysis with mHSF2 are outlined in Fig. 7F. It can be concluded from these results that mHSF2 most likely also binds the HSE through recognition of the dyad symmetry at sites 3 and 4 and that binding to a trimeric site is preferred.

DISCUSSION

mHSF1 and mHSF2 recognize the dyad symmetry of the HSP70 HSE. We have performed a detailed comparison of the DNA binding of mHSF1 and mHSF2 to the HSP70 HSE, a complex binding site composed of five adjacent pentameric sites. We were interested in understanding the nature of mHSF1 and mHSF2 interaction with these sites, what nucleotides were important for binding, and if there was any preference for HSF trimer binding within the HSE. With respect to the latter, the most striking result of these studies came from the missing-nucleoside analysis. The binding of mHSF1 or mHSF2 to gapped DNA in the missing-nucleoside experiment demonstrated that the most sensitive bases in the pentameric binding site were within sites 3 and 4. This can be understood on the basis of a model for HSF interaction with the HSE, in which mHSF1 recognizes the HSE through interactions with the dyad symmetry of sites 3 and 4. Our additional analysis of mHSF1 and mHSF2 binding to dimeric HSEs (data not shown) suggests that this interaction is substantially weaker and that stable binding of HSF occurs when at least three adjacent sites are present. This hypothesis is also supported by the fact that mHSF1 and mHSF2 bind significantly better to a dimeric repeat that contains sites 3 and 4 than to one that does not match the consensus and lacks symmetry.

Our data from the missing-nucleoside experiment also demonstrate that there is a site preference for trimer interaction in binding to the HSE. We found in the mHSF1 complex A that sites 3, 4, and 5 were the preferred binding site for mHSF1. This was concluded because when bases were lost from sites 1 and 2, the formation of complex A was enhanced. This may be functionally important in assembling the transcription complex on the HSP70 gene, as it would permit the binding of two HSF molecules to the HSE. A model for mHSF1 binding to the HSP70 HSE is schematically diagrammed in Fig. 8. The first trimer binds to sites 3, 4, and 5, allowing the binding of a second trimer. The ability of an mHSF1 trimer to bind stably to two sites (1 and 2), as shown at the bottom of Fig. 8, is likely because of the positive cooperative effect exerted by the bound adjacent trimer. Previous analysis of *Drosophila* HSF has also demonstrated the cooperative nature of HSF binding and the preference of HSF for certain sites within the *Drosophila* HSE (41, 56).

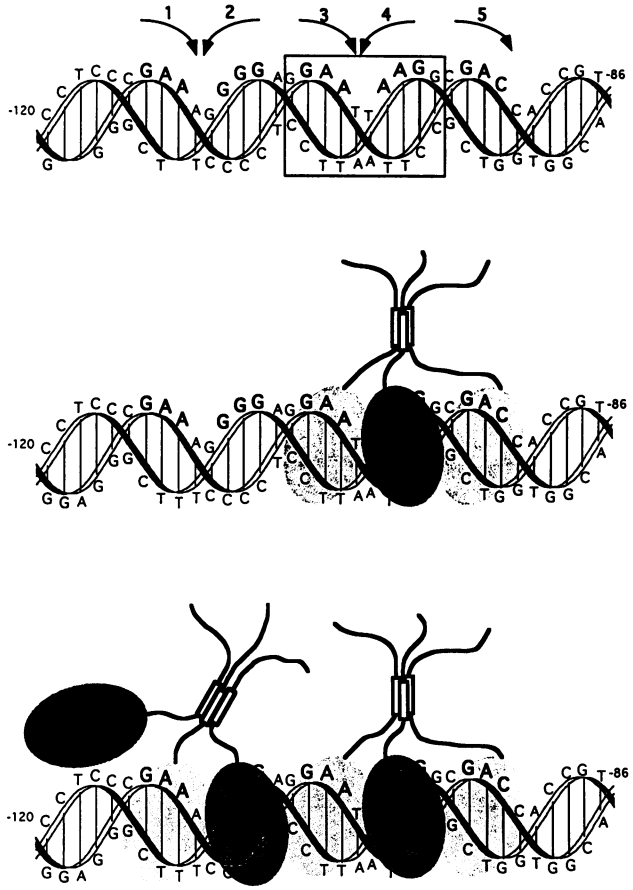

FIG. 8. Model of mHSF1 binding to the HSP70 HSE. The region of the HSE is schematically displayed on a B-form DNA molecule with 10-bp periodicity. At the top, the bases of the HSE region are denoted, and the specific repeats are bolded and denoted with arrows indicating their orientation and number. The box outlines sites 3 and 4 and the 10-bp dyad symmetry. The middle panel shows a trimer of mHSF1 bound to sites 3, 4, and 5. The trimer is drawn as a three-stranded coiled coil; the small boxes represent the oligomerization region. The DNA-binding domains are oval shaped and lie in the major groove of the helix at each site. The dark shadowing indicates that the HSF monomer is in front, and light shadowing indicates that it is behind the helix. At the bottom, the binding of the second mHSF1 trimer at sites 1 and 2 is shown with the adjacent unbound mHSF1 monomer.

The missing-nucleoside experiment also demonstrated that mHSF2 preferred a three-unit binding site. However, we detected differences in mHSF2 interaction that suggest several alternatives for its interaction with the HSE. The binding detected by footprinting may reflect the interaction of a single mHSF2 trimer shifting its interaction between sites 2, 3, and 4 or sites 3, 4, and 5. However, this would lead to only partial protection of sites 2 and 5 during footprinting,

and this is not observed. It is also possible that two mHSF2 trimers interact with the HSE such that each trimer binds to two sites, resulting in the protection of sites 2 to 5. Alternatively, it seems more plausible that one mHSF2 trimer may interact with sites 3, 4, and 5; the weaker interaction of a second trimer at sites 1 and 2 would follow. The binding at site 2 would be stabilized by interactions with site 3, whereas the interaction with site 1 would be weakest, as it has the least opportunity for cooperative interactions.

Analysis of HSF interaction with the HSP70 HSE. Our laboratory has shown that all five consensus G residues of the human HSE are protected from DMS methylation in heat-shocked cells, suggesting that heat-induced HSF1 binds to all five sites (1). We have also shown in our study that mHSF1 protects the same nucleotides in vitro from methylation and that the same DMS hypersensitivities are also present as in vivo. There was evidence from our earlier in vivo study (1) that the protection was stronger at sites 3 and 4, suggesting preferential interaction by HSF1, and this is consistent with our missing-nucleoside analysis. In contrast, DMS protection analysis in hemin-treated K562 cells suggested that HSF2 did not contact the consensus G in HSE site 1 well (42). Our enzymatic and chemical footprinting analysis of mHSF1 and mHSF2 binding addressed the specificity and extent of mHSF1 and mHSF2 binding to the HSP70 HSE. DNase I footprinting demonstrated that mHSF1 bound extensively on both strands and protected all five repeats of the HSE, suggesting that a monomer of mHSF1 was bound to each pentamer. This result is in agreement with previous results that demonstrated that human HSF1 was able to protect the full human HSE (7). This study was limited to analysis of the bottom strand, but similar boundaries were seen. The binding of the *Schizosaccharomyces pombe* HSF protein to the human HSP70 HSE indicated that it also protected all sites, as judged by DNase I footprinting (10). In the same study, methylation interference analysis suggested that the most important interactions of *S. pombe* HSF were at sites 3 and 4. The ability of the yeast protein to bind to the human HSE in nearly the same manner corroborates the conservation observed in the DNA-binding domain of these proteins.

In comparison to mHSF1, our DNase I footprinting analysis of mHSF2 binding demonstrated that sites 2 to 5 were protected and that mHSF2 failed to protect site 1, and these results are consistent with our in vivo study of hemin-induced HSF2 (42). The differences in binding detected by DNase I suggest that mHSF1 and mHSF2 have different affinities for repeats in the HSE. We also demonstrated with MPE footprinting that these two factors protect the DNA backbone primarily in sites 2, 3, and 4. Cunniff et al. (7) also noted that the internal perfect repeats, sites 3 and 4, were better protected by human HSF1 from hydroxyl radical cleavage than the flanking sites. Both mHSF1 and mHSF2 fail to fully protect sites 1 and 5 from hydroxyl radicals, but this might reflect the size of the footprinting reagent. The data suggest that the strength of interaction of a monomer of mHSF1 or mHSF2 with an nGAAn repeat depends on its position within the HSE.

MPE cleavage was significantly lower at the ends of sites 1 and 3 even in the absence of protein, indicative of a narrower minor groove (4). This distortion might be generated by the sequence 5′-AAA-3′ in site 1 and 5′-AATA-3′ in site 3. The bent nature of repeated A tracts in DNA has been demonstrated in other studies (22). However, it seems unlikely that the sequences stated above, although they are appropriately spaced with respect to the helical phase of the DNA, could lead to a significant bend, since they are relatively short. We have attempted to detect bending in this sequence by cloning the HSP70 HSE sequence into the pBEND2 vector (20) and utilizing gel shift analysis. We did not observe an anomalous migration pattern of the free or complexed DNA. The nature and the actual extent of the distortion in the HSE is not known, but it can be speculated that the minor groove of the DNA is narrowed in sites 1 and 3.

mHSF1 and mHSF2 activate transcription and are trimeric in solution. In our studies we have also compared mHSF1 and mHSF2 with respect to their potential for transcriptional activation and oligomeric state. We have utilized concentrations of protein and binding sites that approximate what we know about the concentration and ratio of HSFs to HSEs in vivo (36). Previous studies from our laboratory demonstrated that HSF1 is the factor activated in response to heat and other stresses and that HSF2 is activated in hemin-treated human K562 erythroleukemia cells (36, 42). Our analysis demonstrated that recombinant mHSF1 and mHSF2, both of which are produced in bacteria as active DNA-binding proteins, are trimeric in solution, as judged by EGS cross-linking. This is consistent with previous results from our laboratory and others' regarding the oligomeric state of active HSF (31, 32, 36, 45). We also measured the apparent K_d for the human HSP70 HSE by saturation binding analysis and found that the apparent dissociation constants for mHSF1 and mHSF2 were nearly identical, 2.7 and 2.4 nM, respectively. A previous estimate of the K_d for heat shock-induced *Drosophila* HSF was 4×10^{-12} M (54) and that of human HSF was 4×10^{-11} M (47). It should be noted that our results reflect the binding of recombinant proteins to a natural HSE sequence and that the binding was under different conditions, specifically, those used for transcription and footprinting (notably, higher $MgCl_2$). We also note that the probe used in the analysis of the *Drosphila* and human HSF proteins consisted of multiple consensus nGAAn repeats. It is true that smaller eukaryotes have primarily consensus HSEs, and so the probe is an appropriate substrate for *Drosophila* HSF; however, larger eukaryotes have relatively few perfect HSEs (three adjacent nGAAn sites), and there are multiple HSF factors. Perhaps the divergence of the HSE and the multiplicity of factors in larger eukaryotes has led to a lower binding affinity to permit more versatility in gene regulation. Nevertheless, our analysis suggests that both mHSF1 and mHSF2 bind to the HSE with nearly equal avidity, which is supported by our DNase I footprinting titration, specifically the binding to sites 3 to 5. Both mHSF1 and mHSF2 stimulated transcription in vitro, with mHSF1 being the more potent of the two. This result was consistent with our earlier study that compared heat shock-activated HSF1 and hemin-induced HSF2 (42), although the absolute level of transcriptional activation in vitro is much lower, as has been observed in other studies of recombinant HSFs (6, 33, 40).

Conclusions. How do mHSF1 and mHSF2 bind to DNA, and what are the functional consequences? The primary mode of binding for both proteins is through base contacts in the major groove and with the DNA phosphate-ribose backbone. Both DNase I and DMS treatments of HSF-HSE complexes result in specific hypersensitivities, suggesting that the binding of HSF to the DNA induces some conformational change. The possibility that the HSE is slightly distorted is attractive, as it might help us to visualize how an HSF trimer can bind to a repeat of the sequence 5′-nGAAnnTTCn-3′. For HSF to bind to each site in the major

groove such that the DNA-binding domains are positioned appropriately, the DNA must be distorted to some extent in order to allow symmetrical interactions to occur.

The strong interaction of HSF in vivo with sites 3 and 4 coupled with our missing-nucleoside and gel shift data lead us to speculate that the dyad symmetry of sites 3 and 4 plays a significant role in the recognition of the HSE. Many binding sites for multimeric factors exhibit dyad symmetry that is essential for their interaction with DNA (17, 19). Perhaps the necessity to develop specificity in HSF binding led to the evolution of HSEs with multiple pentameric binding sites. The basic HSE element, 5′-nGAAn-3′, does not lend itself to DNA-binding specificity, as this simple sequence would occur far too frequently in the genome for adequate regulation. The multimerization of the site lends complexity and thus specificity, as well as increased affinity in binding, the latter demonstrated by Xiao et al. (56). To maintain the interaction of HSF with the HSE and allow for the regulated induction of HSF during times of stress, HSF activity has also been regulated at the level of multimerization. Further analysis through binding site selection experiments will address the role of symmetry and base composition in the interaction of HSF with the HSE.

ACKNOWLEDGMENTS

We thank the members of our laboratory and Jonathan Widom for critical review of the manuscript. The expertise and advice of Aseem Ansari and Mark Chael from T. V. O'Halloran's laboratory in chemical footprinting are gratefully acknowledged. We thank David Kroll for suggesting the use of Sarkosyl in mHSF2 purification, Peter Dervan for the gift of MPE (obtained from A. Ansari), Sridhar Rabindran and Carl Wu for the *Drosophila* HSP70 constructs, Sankar Adhya for pBEND2, and Sue Fox for the excellent photography.

This work was supported by NIH grant GM38109 and The March of Dimes (R.I.M.). P. E. Kroeger and K. D. Sarge are recipients of NRSA fellowships from the NIH.

REFERENCES

1. **Abravaya, K., B. Phillips, and R. I. Morimoto.** 1991. Heat shock-induced interactions of heat shock transcription factor and the human *hsp70* promoter examined by in vivo footprinting. Mol. Cell. Biol. **11**:586–592.
2. **Amin, J., J. Ananthan, and R. Voellmy.** 1988. Key features of heat shock regulatory elements. Mol. Cell. Biol. **8**:3761–3769.
3. **Becker, P. B., S. K. Rabindran, and C. Wu.** 1991. Heat shock-regulated transcription in vitro from a reconstituted chromatin template. Proc. Natl. Acad. Sci. USA **88**:4109–4113.
4. **Burkhoff, A. M., and T. D. Tullius.** 1987. The unusual conformation adopted by the adenine tracts in kinetoplast DNA. Cell **48**:935–943.
5. **Cao, Z., R. M. Umek, and S. L. McKnight.** 1991. Regulated expression of three C/EBP isoforms during adipose conversion of 3T3-L1 cells. Genes Dev. **5**:1538–1552.
6. **Clos, J., J. T. Westwood, P. B. Becker, S. Wilson, K. Lambert, and C. Wu.** 1990. Molecular cloning and expression of a hexameric Drosophila heat shock factor subject to negative regulation. Cell **63**:1085–1097.
7. **Cunniff, N. F. A., J. Wagner, and W. D. Morgan.** 1991. Modular recognition of 5-base-pair DNA sequence motifs by human heat shock transcription factor. Mol. Cell. Biol. **11**:3504–3515.
8. **Dynan, W. S.** 1987. DNase I footprinting as an assay for mammalian gene regulatory proteins, p. 75–87. *In* J. Setlow (ed.), Genetic engineering: principles and methods, vol. 9. Plenum Press, New York.
9. **Frankel, S., R. Sohn, and L. Leinwand.** 1991. The use of sarkosyl in generating soluble protein after bacterial expression. Proc. Natl. Acad. Sci. USA **88**:1192–1196.
10. **Gallo, G. J., T. J. Schuetz, and R. E. Kingston.** 1991. Regulation of heat shock factor in *Schizosaccharomyces pombe* more closely resembles regulation in mammals than in *Saccharomyces cerevisiae*. Mol. Cell. Biol. **11**:281–288.
11. **Greene, J. M., and R. E. Kingston.** 1990. TATA-dependent and TATA-independent function of the basal and heat shock elements of a human *hsp70* promoter. Mol. Cell. Biol. **10**:1319–1328.
12. **Greene, J. M., Z. Larin, I. C. Taylor, H. Prentice, K. A. Gwinn, and R. E. Kingston.** 1987. Multiple basal elements of a human *hsp70* promoter function differently in human and rodent cell lines. Mol. Cell. Biol. **7**:3646–3655.
13. **Hayes, J. J., and T. D. Tullius.** 1989. The missing nucleoside experiment: a new technique to study recognition of DNA by protein. Biochemistry **28**:9521–9527.
14. **Hertzberg, R. P., and P. B. Dervan.** 1984. Cleavage of DNA with methidiumpropyl-EDTA-iron(II): reaction conditions and product analyses. Biochemistry **23**:3934–3945.
15. **Hunt, C., and S. Calderwood.** 1990. Characterization and sequence of a mouse hsp70 gene and its expression in mouse cell lines. Gene **87**:199–204.
16. **Jakobsen, B. K., and H. R. B. Pelham.** 1991. A conserved heptapeptide restrains the activity of the yeast heat shock transcription factor. EMBO J. **10**:369–375.
17. **Johnson, P. F., and S. L. McKnight.** 1989. Eukaryotic transcriptional regulatory proteins. Annu. Rev. Biochem. **58**:799–839.
18. **Jones, K. A., K. R. Yamamoto, and R. Tjian.** 1985. Two distinct transcription factors bind to the HSV thymidine kinase promoter in vitro. Cell **42**:559–572.
19. **Jones, N.** 1990. Transcriptional regulation by dimerization: two sides to an incestuous relationship. Cell **61**:9–11.
20. **Kim, J., C. Zwieb, C. Wu, and S. Adhya.** 1989. Bending of DNA by gene-regulatory proteins: construction and use of a DNA bending vector. Gene **85**:15–23.
21. **Kingston, R. E., T. J. Schuetz, and Z. Larin.** 1987. Heat-inducible human factor that binds to a human *hsp70* promoter. Mol. Cell. Biol. **7**:1530–1534.
22. **Koo, H.-S., H.-M. Wu, and D. M. Crothers.** 1986. DNA bending at adenine-thymine tracts. Nature (London) **320**:501–506.
23. **Liu, A. Y., H. S. Choi, Y. K. Lee, and K. Y. Chen.** 1991. Molecular events involved in transcriptional activation of heat shock genes become progressively refractory to heat stimulation during aging of human diploid fibroblasts. J. Cell. Physiol. **149**:560–566.
24. **Maxam, A. M., and W. Gilbert.** 1977. A new method for sequencing DNA. Proc. Natl. Acad. Sci. USA **74**:560–564.
25. **Maxam, A. M., and W. Gilbert.** 1980. Sequencing end-labeled DNA with base-specific chemical cleavages. Methods Enzymol. **65**:499–560.
26. **Morgan, W. D., G. T. Williams, R. I. Morimoto, J. Greene, R. E. Kingston, and R. Tjian.** 1987. Two transcriptional activators, CCAAT-box binding transcription factor and heat shock transcription factor, interact with a human HSP70 gene promoter. Mol. Cell. Biol. **7**:1129–1138.
27. **Mosser, D. D., P. T. Kotzbauer, K. D. Sarge, and R. I. Morimoto.** 1990. In vitro activation of heat shock transcription factor DNA-binding by calcium and biochemical conditions that affect protein conformation. Proc. Natl. Acad. Sci. USA **87**:3748–3752.
28. **Nakai, A., and R. I. Morimoto.** 1993. Characterization of a novel chicken heat shock transcription factor, heat shock factor 3, suggests a new regulatory pathway. Mol. Cell. Biol. **13**:1983–1997.
29. **Nieto-Sotelo, J., G. Wiederrecht, A. Okuda, and C. S. Parker.** 1990. The yeast heat shock transcription factor contains a transcriptional activation domain whose activity is repressed under nonshock conditions. Cell **62**:807–817.
30. **O'Halloran, T. V., B. Frantz, M. K. Shin, D. M. Ralston, and J. G. Wright.** 1989. The MerR heavy metal receptor mediates positive activation in a topologically novel transcription complex. Cell **56**:119–129.
31. **Perisic, O., H. Xiao, and J. T. Lis.** 1989. Stable binding of Drosophila heat shock factor to head-to-head and tail-to-tail

repeats of a conserved 5 bp recognition unit. Cell **59:**797–806.
32. **Peteranderl, R., and H. C. M. Nelson.** Trimerization of the heat shock transcription factor by a triple-stranded α-helical coiled-coil. Biochemistry, in press.
33. **Rabindran, S. K., G. Giorgi, J. Clos, and C. Wu.** 1991. Molecular cloning and expression of a human heat shock factor, HSF1. Proc. Natl. Acad. Sci. USA **88:**6906–6910.
34. **Rosenberg, A. H., B. N. Lade, D.-S. Chui, S.-W. Lin, J. J. Dunn, and F. W. Studier.** 1987. Vectors for selective expression of cloned DNAs by T7 RNA polymerase. Gene **56:**125–135.
35. **Sambrook, J., E. F. Fritsch, and T. Maniatis.** 1989. Molecular cloning: a laboratory manual, 2nd ed. Cold Spring Harbor Laboratory Press, Cold Spring Harbor, N.Y.
36. **Sarge, K. D., S. P. Murphy, and R. I. Morimoto.** 1993. Activation of heat shock gene transcription by HSF1 involves oligomerization, acquisition of DNA binding activity, and nuclear localization and can occur in the absence of stress. Mol. Cell. Biol. **13:**1392–1407.
37. **Sarge, K. D., V. Zimarino, K. Holm, C. Wu, and R. I. Morimoto.** 1991. Cloning and characterization of two mouse heat shock factors with distinct inducible and constitutive DNA-binding ability. Genes Dev. **5:**1902–1911.
38. **Scatchard, G.** 1949. The attractions of proteins for small molecules and ions. Ann. N.Y. Acad. Sci. **51:**660–672.
39. **Scharf, K.-D., S. Rose, W. Zott, F. Schoff, and L. Nover.** 1990. Three tomato genes code for heat stress transcription factors with a remarkable degree of homology to the DNA-binding domain of the yeast HSF. EMBO J. **9:**4495–4501.
40. **Schuetz, T. J., G. J. Gallo, L. Sheldon, P. Tempst, and R. E. Kingston.** 1991. Isolation of a cDNA for HSF2: evidence for two heat shock factor genes in humans. Proc. Natl. Acad. Sci. USA **88:**6910–6915.
41. **Shuey, D. J., and C. S. Parker.** 1986. Binding of Drosophila heat-shock transcription factor to the hsp 70 promoter: evidence for symmetric and dynamic interactions. J. Biol. Chem. **261:** 7934–7940.
41a. **Sistonen, L.** Unpublished data.
42. **Sistonen, L., K. D. Sarge, B. Phillips, K. Abravaya, and R. Morimoto.** 1992. Activation of heat shock factor 2 during hemin-induced differentiation of human erythroleukemia cells. Mol. Cell. Biol. **12:**4104–4111.
43. **Sorger, P. K.** 1990. Yeast heat shock factor contains separable transient and sustained response transcriptional activators. Cell **62:**793–805.
44. **Sorger, P. K., M. J. Lewis, and H. R. B. Pelham.** 1987. Heat shock factor is regulated differently in yeast and HeLa cells. Nature (London) **329:**81–84.
45. **Sorger, P. K., and H. C. M. Nelson.** 1989. Trimerization of a yeast transcriptional activator via a coiled-coil motif. Cell **59:**807–813.
46. **Studier, F. W., and B. A. Moffat.** 1986. Use of bacteriophage T7 RNA polymerase to direct selective high-level expression of cloned genes. J. Mol. Biol. **189:**113–130.
47. **Taylor, I. C. A., J. L. Workman, T. J. Schuetz, and R. E. Kingston.** 1991. Facilitated binding of GAL4 and heat shock factor to nucleosomal templates: differential function of DNA-binding domains. Genes Dev. **5:**1285–1298.
48. **Tullius, T. D., B. A. Dombroski, M. E. A. Churchill, and L. Kam.** 1987. Hydroxyl radical footprinting: a high-resolution method for mapping protein-DNA contacts. Methods Enzymol. **155:**537–558.
49. **Westwood, J. T., J. Clos, and C. Wu.** 1991. Stress-induced oligomerization and chromosomal relocalization of heat-shock factor. Nature (London) **353:**822–827.
50. **Wiederrecht, G., D. Seto, and C. S. Parker.** 1988. Isolation of the gene encoding the S. cerevisiae heat shock transcription factor. Cell **54:**841–853.
51. **Williams, G. T., T. K. McClanahan, and R. I. Morimoto.** 1989. E1a transactivation of the human HSP70 promoter is mediated through the basal transcriptional complex. Mol. Cell. Biol. **9:**2574–2587.
52. **Williams, G. T., and R. I. Morimoto.** 1990. Maximal stress-induced transcription from the human *hsp70* promoter requires interactions with the basal promoter elements independent of rotational alignment. Mol. Cell. Biol. **10:**3125–3136.
53. **Wu, B. J., R. E. Kingston, and R. I. Morimoto.** 1986. Human HSP70 promoter contains at least two distinct regulatory domains. Proc. Natl. Acad. Sci. USA **83:**629–633.
54. **Wu, C., S. Wilson, B. Walker, I. Dawid, T. Paisley, V. Zimarino, and H. Ueda.** 1987. Purification and properties of *Drosophila* heat shock activator protein. Science **238:**1247–1253.
55. **Xiao, H., and J. T. Lis.** 1988. Germline transformation used to define key features of the heat shock response element. Science **239:**1139–1142.
56. **Xiao, H., O. Perisic, and J. T. Lis.** 1991. Cooperative binding of Drosophila heat shock factor to arrays of a conserved 5 bp unit. Cell **64:**585–593.